Adsorption of Azo Dye Onto TiO₂ Nanoparticles Prepared by a Novel Green Method: Isotherm and Thermodynamic Study

Rasha Tariq Salim* , Dunya Edan AL-Mammar
Department of Chemistry, College of Science, University of Baghdad, Baghdad, Iraq

Abstract

The current study examined the use of Sansevieria plant leaves extract as an environmentally acceptable, inexpensive, and safe green approach for creating titanium dioxide nanoparticles (NPs). Batch studies have been used to test the particles' capacity to bind to the azo dye congo red (CR), which has been adsorbed from its aqueous solution. The effects of many factors, including the weight of TiO2 NPs, the contact duration to reach equilibrium, the concentration of CR, temperature, and pH, have been investigated. Both the Freundlich and Langmuir models were used to analyze experimental results. According to the high values of the Freundlich model's correlation coefficient R^2, it is discovered that the adsorption of CR dye onto nano TiO₂ is well-suited. The kinetics analysis for the adsorption trials proposed the pseudo-second-order. Thermodynamic data showed that the CR dye adsorption onto nano TiO₂ is a physical process that happens spontaneously and endothermically with increasing unpredictability.

Keywords: Adsorption, azo dye, TiO₂ NPs, Isotherm, Thermodynamic**,** a novel green method**.**

امتزاز صبغة الآزو على دقائق أوكسيد التيتانيوم النانوية المحضرة بطريقة خضراء جديدة : دراسة متساوي درجة الحرارة والدينمية الحرارية

رشا طارق سالم* , دنيا عيدان المعمار
قسم الكيمياء , كلية العلوم , جامعة بغداد , بغداد , العراق

الخلاصة

تبحث الدراسة الحالية في استخدام مستخلص أوراق السنسفيرا كطريقة خضراء صديقة للبيئة , رخيصة وغير سامة لتخليق دقائق أوكسيد التيتانيوم النانوية. قابلية امتزاز هذه الدقائق لأمتزاز صبغة الآزو كونغو الحمراء (CR) من محاليلها المائية تم اجراءها بأستخدام تجارب الوجبة . تم دراسة تأثير مختلف الظروف مثل وزن دقائق أوكسيد التيتانيوم النانوية , زمن الرج , تركيز صبغة الكونغو الحمراء , درجة الحرارة والأس الهيدروجيني . النتائج التجريبية أختبرت طبقاً الى إنموذجي لنكماير وفرندلش . لقد وجد ان امتزاز صبغة الكونغو الحمراء على سطح أوكسيد التيتانيوم النانوي جيد التطابق مع إنموذج فرندلش طبقاً الى قيمة معامل الأرتباط R² العالية . الدراسة الحركية لتجارب الأمتزاز تقترح كون عملية الأمتزاز تتبع المرتبة الثانية المنتحلة . النتائج الثرمودينمكية

---

* Email: rashatariq46@gmail.com

تشير الى ان عملية امتزاز صبغة الكونغو الحمراء على سطح اوكسيد التيتانيوم النانوية هو عملية امتزاز فيزيائي

تلقائي , ماص للحرارة ويحدث مع زيادة العشوائية . ,

1- Introduction

Wastewater is a significant contributor to environmental pollution since it is a byproduct of the use of water in homes, companies, and enterprises [1]. Since a lot of dye waste is dumped into rivers, causing significant environmental harm, dyes are a substantial source of water pollution [2]. The decolourization of the dyes in industrial wastewater involved various techniques. These techniques of treatment consist of ultrafiltration [3], ion-exchange [4], electro-chemical-degradation [5], photo catalytic degradation [6, 7] and adsorption process [8]. The adsorption of dye onto nanoparticles was the most practical approach since it is straightforward, highly efficient, and can use a variety of materials as adsorbents [9]. Adsorption refers to a solid's capacity to accumulate other substances from solution on its surfaces. Many materials have been employed as adsorbents for decolorizing industrial wastewater, including raw with activated illite mixed, chlorite and kaolinite [10], modified bentonite [11] and Thuja plant [12]. TiO$_2$ nanomaterials are now regarded as a promising material that is heavily involved in getting rid of toxic organic containments through the adsorption and photo-catalytic process due to the stability of its structure, bio-compatibility, strong oxidizing agent, [13] and non-toxicity of the metal precursors [14-19]. TiO$_2$ nanoparticles were previously used frequently for the treatment of textile effluents. TiO$_2$ nanoparticles are produced using a variety of techniques, including biosynthesis, sol-gel process, and plasma-enhanced chemical vapour deposition (PE-CVD). TiO$_2$ nanoparticle biosynthesis is receiving a lot of attention due to its ease of usage, low cost, and lack of toxicity [20]. As a result, plant and herbal extracts are increasingly appealing due to the easier and more cost-effective process and the inclusion of ingredients including flavonoids, terpenoids, and polysaccharides [21].

The objectives of this work was to synthesize TiO$_2$ nanoparticles utilizing a unique biosynthesis technique based on a leaf extract from the Sansevieria plant. Additionally, this study assessed the efficiency of these synthesized nanomaterials to adsorb CR dye from solution. The effects of several variables, including the weight of TiO$_2$ NPs, the contact time required to reach equilibrium, the initial concentration of CR, temperature, and pH, were investigated. To comprehend the mechanism of the adsorption process, kinetic, thermodynamic, and adsorption isotherm models were studied.

2. Experimental part
2.1. Materials

Adsorbent: Titanium dioxide nanoparticles were synthesized using an extract from Sansevieria plant leaves, which were bought from a local market. The leaves of this plant were cut, thoroughly washed with tap water, and then repeatedly cleaned with D.W. to get rid of any remaining dust and grime. A 100 mL of boiling, distilled water was combined with 25 g of finely chopped plant material, and the mixture was continually heated for 2 hours at 90 °C. Using No. 1 filter paper, the plant extract was filtered. A 2.8 mL of titanium tetrachloride was added to 100 mL of distilled water as a precursor, and the mixture was well agitated. The previously produced Sansevieria plant leaf extract was gradually added to the titanium tetrachloride solution while being continuously stirred. For four hours, the mixture was continually stirred. The precipitate was regularly calcined at 500 °C for 4 hours after being dried at 100 °C for 24 hours. The precipitate will be rinsed with D.W many times to remove the contaminants. The titanium dioxide nanoparticles were then obtained as a white precipitate after being heated at 700 oC for an hour. The precipitate was then crushed in a lab mill and kept in a

dry area. Utilizing XRD (XRD, PW1730, Philips, Holanda) analysis, the synthesized TiO_2 was identified. The data collected for TiO_2 powder showed that the average crystalline size was 15.2 nm. Atomic force microscopy AFM (Nano AFM 2022, Nanosurf, Switzerland) measurements indicated that TiO_2 sample has a small size distribution with a diameter of 67.73 nm. TiO_2-NPs were investigated by FTIR spectroscopy (Shimadzu IR-Affinity-1 Japan). The metal-oxygen bonding is confirmed by the peaks that are characteristic of the Ti-O bending mode of vibration, which has a center frequency of 497.63 and 688.59 cm^{-1}. The Ti-O stretching bands are described by the sharp peak between 800 and 450 cm^{-1} . The morphology of the prepared TiO_2 was detected by scanning electron microscopy SEM using (FESEM-EDS, MIRA III, TESCAN, Czech), the particle size of TiO_2-NPs was found to be 42.039 nm. Figure 1 shows the steps of TiO_2 NPs preparation [22].

Figure 1: Steps used for sytnehsis of TiO_2 NPs using Sansevieria plant leaves.

Adsorbate:

Congo red (CR), an anionic dye or acidic dye, with a molar mass of 696.665 g/mole and the chemical formula $C_{32}H_{22}N_6Na_2O_6S_2$. Disodium 4-amino-3-[4-[4-[4-(1-amino-4-sulfonato-naphthalene-2-yl) diazinyl-phenyl]phenyl]diazenyl-naphthalene-1-sulonate is the compound's IUPAC nomenclature. The highest absorption of this dye is 497 nm, making it useful as a substitute indicator to mimic contamination in industrial wastewater [23]. The chemical structure of this dye is shown in Figure 2.
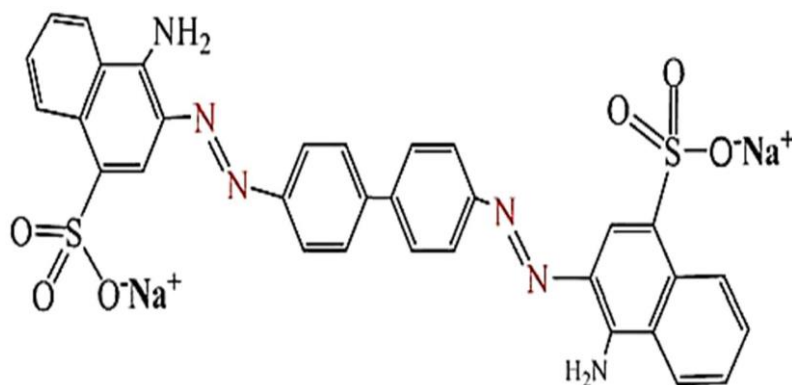
Figure 2: Chemical structure of congo red CR dye.

2.2. Adsorbate preparation:

One gram of the CR dye was diluted with one liter of distilled water to prepare the stock solution. To prepare different CR dye concentrations, 10, 20, 30, 40, and 50 mg/L, the stock solution was further diluted. The absorbance of each solution is measured using UV-Vis spectrophotometer (Shimadzu UV-1800) Japan.

2.3. Adsorption Experiments:

Using the batch equilibrium approach, adsorption experiments were conducted. In a 25 mL CR solution that was placed in a 100 mL conical flask, a specific weight of TiO_2 NPs sample was added. Then, the mixture was shaken with a thermostatic water bath of the JTYS-1000 design from China at a speed of 150 rpm for 60 minutes at various temperatures. The residual CR dye concentration was determined using a Shimadzu UV-1800 UV-Vis Spectrophotometer after 10 minutes of centrifugation at 4000 rpm to separate the adsorbent.

The removal percentage (R%) for CR and the amount of the adsorbed dye (qe) in mg.g^{-1} were estimated as the following relations [24]:

$$R \% = \left[\frac{C_i - C_e}{C_i} \right] 100 \tag{1}$$

$$q_e = V/ w \left[C_i - C_e \right] \tag{2}$$

C_i , C_e are the initial concentration and the equilibrium concentration mg/L, V is the working solution volume (L) and w is the weight of TiO_2 NPs sample (g). The kinetics study for the adsorption of CR on TiO_2 NPs was carried out using 25 mL of 10 mg/L CR dye solution under the following conditions: the adsorption time (10, 20, 30, 40, 50, 60) minutes, pH equals to 7, shaking speed 150 rpm at five different temperatures of (288 to 328) K, in a set of 100 mL conical flasks. A 1.0 mL of the supernatant was taken out every five, ten, twenty, thirty, forty, fifty, and sixty minutes until the dye reached equilibrium. At a speed of 4000 rpm, the liquid and solid phases were separated for five minutes. The supernatant was analyzed to determine the adsorbate concentration using UV-Vis spectrophotometer (Shimadzu UV-1800) Japan.

3. Results and Discussions
3.1. Impact of TiO_2 NPs weight

Various amounts of TiO_2 NPs in the range of (0.05 to 0.3) g and 25 mL of 10 mg/L CR dye were used in experiments to determine the effect of the TiO_2 NPs weight on the removal % of the CR dye. The conditions were 298 K, pH = 7, and 150 rpm shaking. According to Figure 3, when the weight of TiO_2 NPs increased, the R% for CR dye increased from 39.09 to 96.10%.

The availability of more adsorption sites for CR dye was increased by the elevation in R% values [25]. As a consequence, 0.2 g is selected as the optimum mass for further studies with the help of the prior finding.
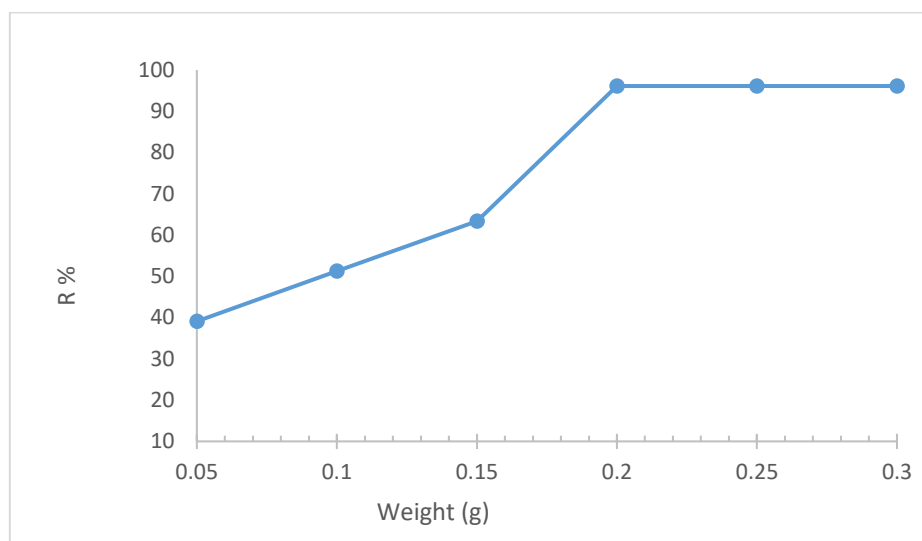
Figure 3: Effect of TiO$_2$ NPs weight on the R% of CR dye.

3.2. Effect of contact time

The effect of altering the CR dye adsorption duration from 5 to 80 minutes was determined while maintaining other parameters such pH 7, starting CR concentration of 10 mg/L, TiO$_2$ NPs weight of 0.2 g, and 150 rpm shaking speed at 298 K. The effects of agitation time on the adsorption of CR dye are shown in Figure 4. The proportion of removal in this figure increases with passing time and reaches equilibrium in around 60 minutes, after which the rate of removal remains constant. This might be a reference to the possibility of CR molecules adhering to a wide surface area on all adsorbents for at least 60 minutes after the unoccupied surface sites have been saturated, because of this, the removal efficiency is unaffected. Thus, 60 minutes was chosen as the optimum time period.
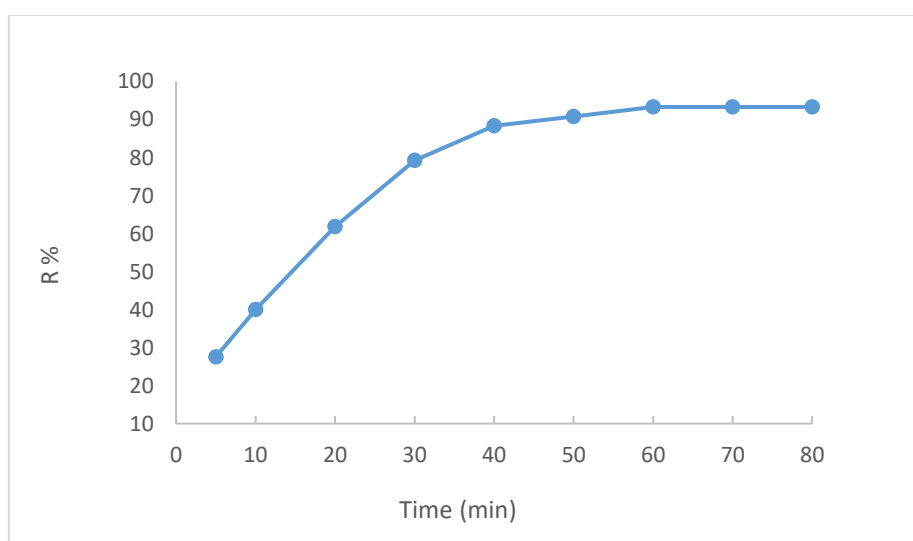
Figure 4: Effect of contacting time on the adsorption of CR dye on TiO$_2$ NPs.

3.3. Effect of initial concentration on the adsorption process

The impact of starting CR concentration on the adsorption were experimentally examined at CR concentration ranging (10, 20, 30, 40, and 50) mg/L, TiO$_2$ NPs weight under following experimental conditions: 0.2 g, pH equals to 7, at 298K , contact time 60 minutes and 150 rpm of shaking speed. The values of the adsorption dye q e (mg/g) increased from (1.246 to 4.838) mg/g when the CR concentration increased, according to Figure 5a. This was linked to a significant probability of dye molecule collision with surfaces of TiO$_2$ NPs, together with a high rate of dye diffusion onto adsorbent surface [26]. Further, Figure 5b demonstrates that when beginning CR concentration increased, the R% for CR fell from (93.92 to 56.79)%. The increased absorption of CR dye at low concentrations suggests the potential of more binding sites on the surface of TiO$_2$ NPs for less CR, which may be connected to the lack of viable binding sites necessary for the high beginning CR concentration [27]. Figure 5a shows the relation between the starting CR concentration and the adsorption amount q_e.
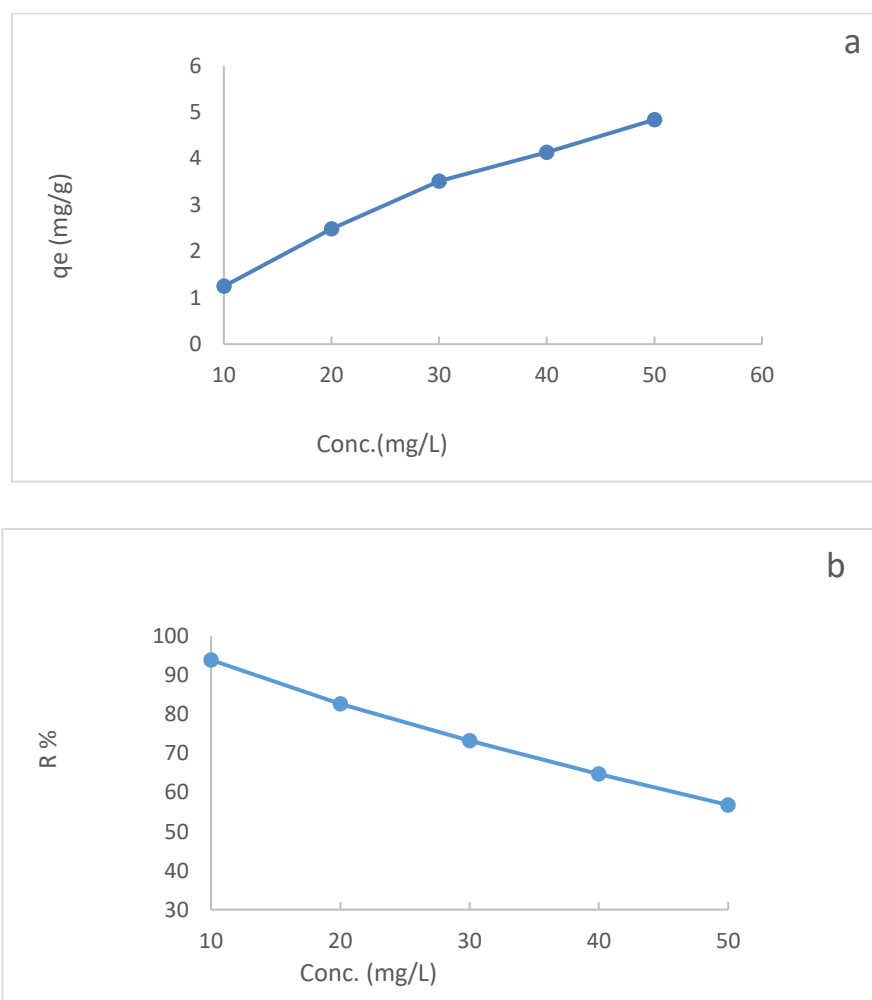
Figure 5: Effect of initial concentration of CR on the adsorption of CR dye on TiO$_2$ NPs. (a) Adsorption capacity q_e (mg/g). (b) Removal efficiency R%.

3.4. Effect of temperature on adsorption of CR dye on TiO$_2$ NPs

By adjusting the temperature from (288 K to 328 K), it was possible to determine the percentage of CR dye that was removed using TiO$_2$ NPs samples. The studies involved mixing 25 mL of 10 mg/L CR solutions with 0.2 g of TiO$_2$ NPs for 60 minutes at a speed of 150 rpm. The effect of temperature on CR dye adsorption on TiO$_2$ NPs is shown in Figure 6. This Figure demonstrates that raising the temperature from (288 K to 328 K) causes the percentage removal

to grow before stabilizing at a constant value, which is why the adsorption process has been categorized as an endothermic process [28]. This can be because the sorption process occurred.
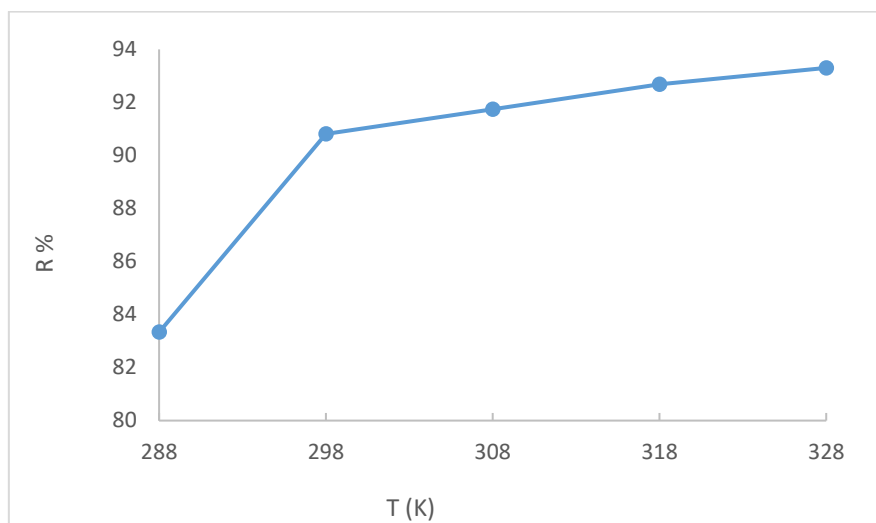
Figure 6: Effect of temperature on the adsorption of CR on TiO_2 NPs.

3.5. pH effect

The removal of CR using a sample of TiO_2 NPs is examined in the pH range of (2.6-10.8) at 298 K, initial CR concentration of 10 mg/L, 0.2 g weight of TiO_2 NPs, 60 min of shaking time and 150 rpm of shaking speed. Figure 7 shows that the amount of CR dye removed by TiO_2 NPs has decreased from (97 to 58)% when the pH values changed from (2.6 to 10.8). This can be explain by the following fact due to the high positive charge density on the adsorbent's surface, the adsorption of the anionic CR dye can be increased in an acidic media. When the pH is lower, the increase in H+ concentration in TiO_2 NPs generates a positive charge through H+ adsorption, which causes the adsorption of CR dye to increase. Since TiO_2 NPs are positively charged in an acidic environment, they exhibit a high electrostatic attraction to CR aions, leading to the maximal elimination of the CR dye. While this is happening, the number of negatively charged sites that are unfavorable for the adsorption of CR dye molecules due to electrostatic repulsion is expanding as pH values increase [29].
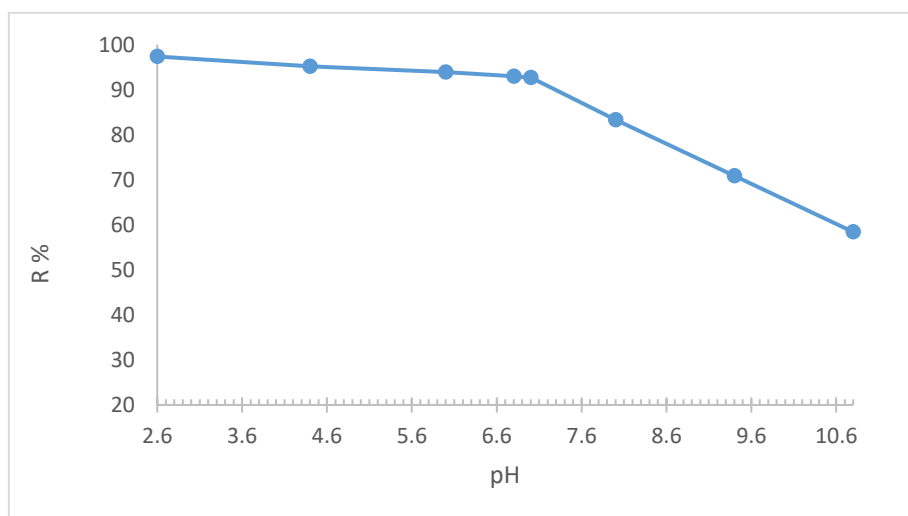
Figure 7: Effect of pH on the adsorption of CR dye on TiO_2 NPs.

3.6. Adsorption Isotherm Models

To describe the type of interaction and equilibrium relationship between the TiO_2 NPs surface and CR dye molecules, the isotherm models is applied [30].

3.6.1. Langmuir isotherm model:

Based on the formation of uniform and a homogenous sites for adsorption, Langmuir linear forms is presented by following the equation [31]:

$$\frac{C_e}{q_e} = \frac{1}{K_L\, Q_m} + \frac{1}{Q_m}\cdot C_e \tag{3}$$

Where C_e CR equilibrium concentration mg/L, q_e amount of the adsorbate that adsorbed per g of the adsorbent at equilibrium mg/g, Q_m maximum adsorption capacity of the mono-layer coverage mg/g and K_L Langmuir isotherm constant $L.mg^{-1}$. The calculated parameters are listed in Table1.

Where the values of Q_m and K_L are estimated from the slope and intercept of the line obtained from drawing C_e/q_e versus C_e as shown in Figure 8. The fundamental characteristic can also be indicated by Langmuir's equation in terms of a dimensionless constant, R_s is the separation factor expressed as:

$$R_s= 1/\ (1 + K_L\ C_i) \tag{4}$$

Where C_i is the initial concentration ($mg.L^{-1}$). The R_s values suggested the shap of the isotherm to be either linear $R_s=1$, favorable $0 < R_s < 1$, unfavorable $R_s > 1$ or irreversible $R_s = 0$ [32]. The obtained values are given in Table 1. The R_s values are less than one and greater than zero show a favorable adsorption.
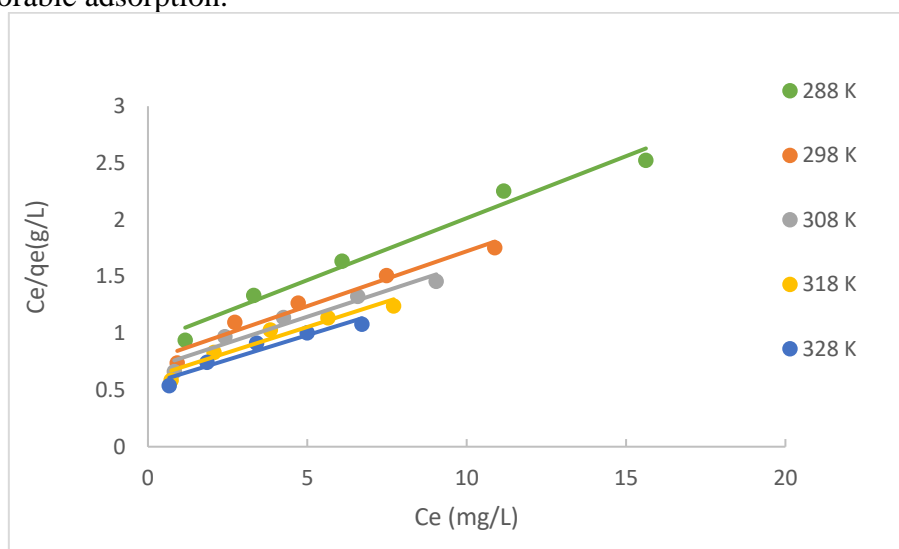
Figure 8: Langmuir isotherms of CR dye on TiO_2 NPs at various temperatures.

Table 1: Langmuir constants data for adsorption of CR dye on TiO_2 NPs at various temperatures.

Temperature (K)	Q_m (mg.g^{-1})	K_L (L/mg)	R^2	R_S
288	9.157509	0.118515	0.9762	0.457634
298	10.341260	0.128063	0.9608	0.438476
308	10.845990	0.134736	0.9420	0.426010
318	11.111110	0.148810	0.9301	0.401914
328	11.534030	0.157780	0.9265	0.387920

3.6.2. Freundlich isotherm:

This model deals with multilayer, non-ideal, reversible adsorption onto heterogeneous energy surface system [30]. The linear form of this model can be experssed as [33]

$$\ln q_e = \ln K_{Fr} + \left(\frac{1}{n_f}\right)\ln C_e \qquad (5)$$

Where: C_e (mg/L) is the equilibrium concentration, K_{Fr} is Freundlich constant indicated to adsorption capacity, and n_f constant that depended on the temperature and the adsorbate nature. The values of K_{Fr} and n_f can be estimated from the linear plot $\ln q_e$ versus $\ln C_e$ as shown in Figure 9. These values are listed in Table 2. When $\frac{1}{n_f}$ equals to 1, the curve of the adsorption is linear which indicates no interaction between the CR species and the adsorbent sites. While when $\frac{1}{n_f}$ greater than 1, the adsorption is not favorable, the adsorption capacity decreases and the bonds of adsorption become weak. Whereas, $\frac{1}{n_f}$ less than 1 the adsorption capacity shows an increase and the adsorption is then favorable [34].
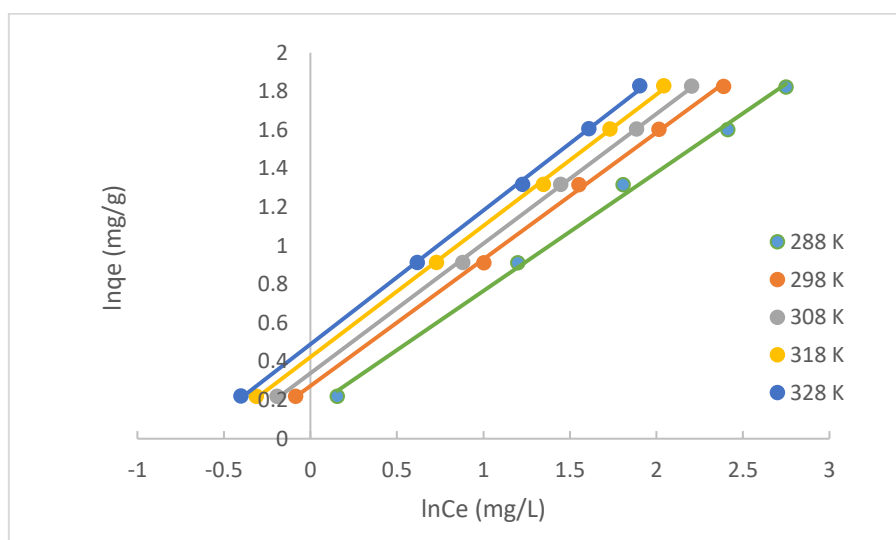
Figure 9: Freundlich isotherm plot for the adsorption of CR on TiO$_2$ NPs at various temperatures.

Table 2: The values of Freundlich isotherm data at various temperatures for the adsorption of CR dye on TiO$_2$ NPs.

Temperature (K)	Slope $(\frac{1}{n_f})$	n_f	Intercept lnK_{Fr}	K_{Fr} $(mg.g^{-1}(mg.L^{-1})^{-1/n})$	R^2
288	0.6133	1.630523	0.1524	1.164626	0.9965
298	0.6562	1.523926	0.2734	1.314426	0.9992
308	0.6720	1.488095	0.3391	1.403684	0.9997
318	0.6802	1.470156	0.4229	1.526382	0.9995
328	0.6937	1.441545	0.4892	1.631011	0.9994

3.7. Thermodynamic Study:

Thermodynamic data such as Gibbs free energy $\Delta G°$, standard enthalpy changes $\Delta H°$ and standard entropy changes $\Delta S°$ were estimated using the following equations :

$$\Delta G° = -RTlnK_{eq} \tag{6}$$

$$K_{eq} = \frac{C_i-C_e}{C_e} \ [V/m] \tag{7}$$

$$\Delta G° = \Delta H° - T\Delta S° \tag{8}$$

Where: K_{eq} is the equilibrium constant for the adsorption process, R: is the universal gas constant, T: absolute temperature (K), C_i and C_e: are the initial and the equilibrium concentrations (mg/L) of the adsorbate, respectively, V: is the CR solution's volume (L) and m: is the mass of the TiO$_2$ NPs (g). The standard entropy $\Delta S°$ and enthalpy $\Delta H°$ can be calculated from the intercept and the slope of the line between lnK_{eq} versus 1/T using Van't Hoff equation [35]: as shown in Figure 10 :

$$lnK_{eq} = \frac{\Delta S°}{R} - \frac{\Delta H°}{RT} \tag{9}$$

Values of the thermodynamic data are given in Table 3. At all temperatures, the values of $\Delta G°$ are negative and it become more negative when the temperature has increased. This finding suggested that at high temperature the adsorption of CR onto TiO$_2$ NPs being more spontaneous. While the positive values of $\Delta S°$ and $\Delta H°$ give an indication that this process endothermic a ccompained with increase in the disorder [36]. Since the values of $\Delta G°$ less than 20 kJmol^{-1}, it can be predicted that the adsorption process followed physisorption type [37].
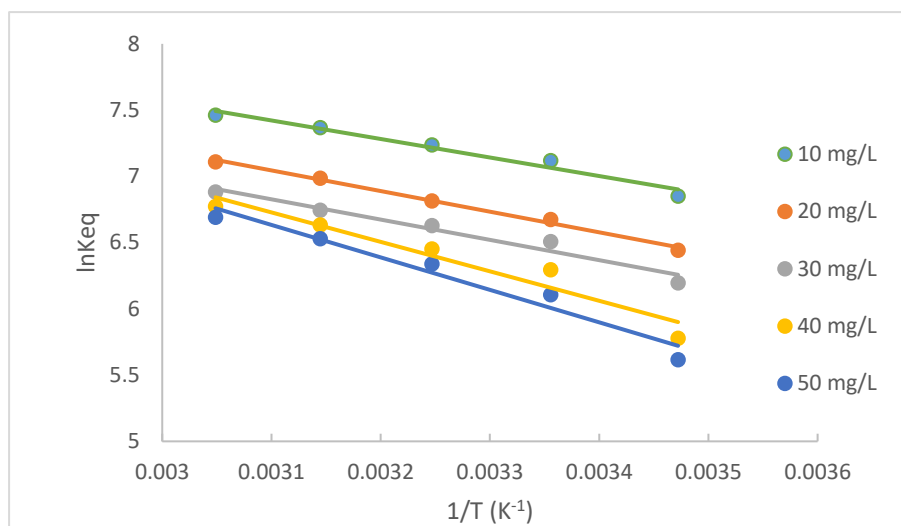
Figure 10: Van't Hoff plots for the adsorption of CR dye on TiO_2 NPs.

Table 3. Thermodynamic parameters for the adsorption of CR dye on TiO_2 NPs.

C_i (mg/L)	ΔH^o(kJ/mol)	ΔS^o(J/mol)	(-) ΔG^o(kJ/mol)				
			288K	**298K**	**308K**	**318K**	**328K**
10	11.62214	97.73107	16.4047	17.6377	18.5305	19.4765	20.3498
20	12.94906	98.71212	15.4282	16.5372	17.4486	18.4709	19.3880
30	12.72624	96.20961	14.8356	16.1206	16.9754	17.8325	18.7664
40	18.48452	113.2367	13.8320	15.5986	16.5213	17.5351	18.4733
50	20.37346	118.3082	13.4494	15.1308	16.2296	17.2652	18.2492

3.8. Kinetics of Adsorption:

In this study, two different kinetic models: Pseudo first order (PFO) and Pseudo second order (PSO) have been applied.

The linearized PFO and PSO models written respectively as equations [38]:

$$\ln (q_e\text{-}q_t) = \ln q_e - k_1.t \tag{10}$$

$$\frac{t}{q_t} = \frac{1}{k_2\,q_e^2} + \frac{t}{q_e} \tag{11}$$

Where q_t, q_e are the a mount of CR dye molecules adsorbed on the TiO_2 NPs at time t and at equilibrium (mg/g). k_1 (min^{-1}), k_2 (g.mg^{-1}.min^{-1}) are the rate constants of PFO and PSO respectively. The linear plot of $\ln (q_e - q_t)$ versus (t) and t/q_t versus t are employed to calculate k_1, q_e values for PFO and k_2, q_e for PSO as shown in Figures 11 and 12. Table 4 lists the PFO and PSO constants for the adsorption process. As shown in Table 4, the values of correlation coefficient R^2 for PSO were higher than that for PFO also, the values of q_e experimental $q_{e\,exp}$ and q_e calculated $q_{e\,cal}$ were matched well using PSO kinetic models, suggesting that the mechanisms of the adsorption related to the both adsorbent and adsorbate [39].
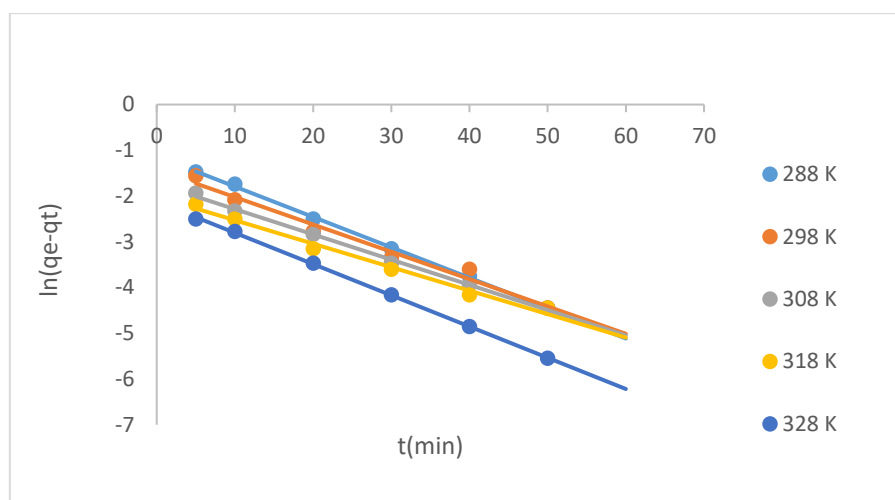
Figure 11: PFO plot of kinetics of CR dye on TiO_2 NPs at various temperatures.
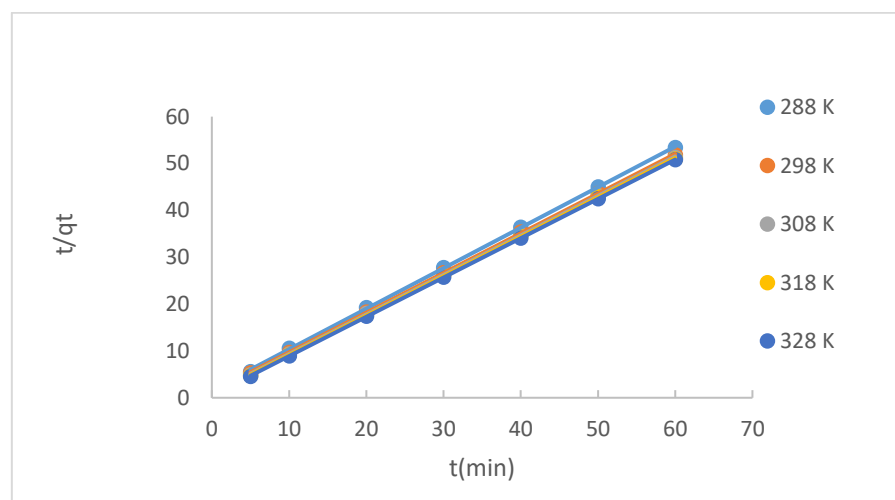
Figure 12: PSO plot for the adsorption of CR on TiO_2 NPs at various temperatures.

Table 4. PFO and PSO kinetics data for adsorption of CR dye on TiO_2 NPs at various temperatures.

T (K)	$q_{e\ exp}$ (mg/g)	$q_{e\ cal}$ (mg/g)	k_1 (min^{-1})	R^2	$q_{e\ exp}$ (mg.g^{-1})	$q_{e\ cal}$ (mg.g^{-1})	k_2 (g/mg.min)	R^2
288	1.123442	0.323389	0.0664	0.9990	1.123442	1.155936	1.6938	0.9998
298	1.158489	0.240172	0.0598	0.9785	1.158489	1.180777	1.2226	0.9999
308	1.170171	0.176524	0.0552	0.9967	1.170171	1.185536	0.9094	0.9999
318	1.177960	0.133214	0.0513	0.9879	1.177960	1.188778	0.6965	0.9999
328	1.181854	0.119864	0.0683	0.9996	1.181854	1.192037	0.4999	1.0000

Conclusion

From this study, it can be observed that CR dye may be effectively removed from its aqueous medium utilizing TiO_2 NPs that were synthesized using Sansevieria plant leaves extract. The Freundlich isotherm was the most effective model for the data at equilibrium. PSO model served as a better representation of the kinetic investigation. The adsorption of CR onto TiO_2 NPs was physisorption, endothermic and it spontaneously occurs as the randomization increases.

References

[1] H. H. Kadhim and K. A. Saleh, "Removing of Copper ions from Industrial Wastewater Using Graphene oxide/Chitosan Nanocomposite," *Iraqi Journal of Science,* pp. 1894-1908, 2022.

[2] M. T. Yagub, T. K. Sen, S. Afroze, and H. M. Ang, "Dye and its removal from aqueous solution by adsorption: a review," *Advances in colloid and interface science,* vol. 209, pp. 172-184, 2014.

[3] T. Lakdioui, A. Essamri, and A. El Harfi, "Optimization study of ultrafiltration rate of a membrane based on polysulfone modified titanium dioxide on coloured water by indigo," *J Mater Environ Sci,* vol. 8, no. 11, pp. 4052-4056, 2017.

[4] J. Ran, L. Wu, Y. He, Z. Yang, Y. Wang, C. Jiang, and T. Xu, "Ion exchange membranes: New developments and applications," *Journal of Membrane Science,* vol. 522, pp. 267-291, 2017.

[5] M. Morsi, A. Al-Sarawy, and W. S. El-Dein, "Electrochemical degradation of some organic dyes by electrochemical oxidation on a Pb/PbO$_2$ electrode," *Desalination and Water Treatment,* vol. 26, no. 1-3, pp. 301-308, 2011.

[6] M. Abbas and M. Trari, "Removal of methylene blue in aqueous solution by economic adsorbent derived from apricot stone activated carbon," *Fibers and Polymers,* vol. 21, no. 4, pp. 810-820, 2020.

[7] M. Abbasa and M. Trarib, "Photocatalytic degradation of Asucryl Red (GRL) in aqueous medium on heat-treated TiO," *Desalination and Water Treatment,* pp. 398-404, 2020.

[8] M. Abbas, A. Cherfi, S. Kaddour, and T. Aksil, "Adsorption in simple batch experiments of Coomassie blue G-250 by apricot stone activated carbon—Kinetics and isotherms modelling," *Desalination and Water Treatment,* vol. 57, no. 32, pp. 15037-15048, 2016.

[9] M. Abbas, Z. Harrache, and M. Trari, "Removal of gentian violet in aqueous solution by activated carbon equilibrium, kinetics, and thermodynamic study," *Adsorption Science & Technology,* vol. 37, no. 7-8, pp. 566-589, 2019.

[10] S. A. Saed and D. E. AL-Mammar, "Influence of Acid Activation of a Mixture of Illite, Koalinite, and Chlorite Clays on the Adsorption of Methyl Violet 6B Dye," *Iraqi Journal of Science,* pp. 1761-1778, 2021.

[11] D. E. Al-Mammar, "Removal of Birlliant Green Dye From Aqueous Solution by Adsorption Onto Modified Clay," *Ibn AL-Haitham Journal For Pure and Applied Science,* vol. 26, no. 2, pp. 206-219, 2017.

[12] D. E. Al-Mammar, "Decolorization of the aqueous Safranin O dye solution using Thuja orientalis as biosorbent," *Iraqi Journal of Science,* vol. 55, no. 3A, pp. 886-898, 2014.

[13] M. Abbas, "Experimental investigation of activated carbon prepared from apricot stones material (ASM) adsorbent for removal of malachite green (MG) from aqueous solution," *Adsorption Science & Technology,* vol. 38, no. 1-2, pp. 24-45, 2020.

[14] M. Abdel-Messih, M. Ahmed, and A. S. El-Sayed, "Photocatalytic decolorization of Rhodamine B dye using novel mesoporous SnO$_2$–TiO$_2$ nano mixed oxides prepared by sol–gel method," *Journal of Photochemistry and Photobiology A: Chemistry,* vol. 260, pp. 1-8, 2013.

[15] M. Ahmed, "Synthesis and structural features of mesoporous NiO/TiO$_2$ nanocomposites prepared by sol–gel method for photodegradation of methylene blue dye," *Journal of Photochemistry and Photobiology A: Chemistry,* vol. 238, pp. 63-70, 2012.

[16] M. Ahmed, E. E. El-Katori, and Z. H. Gharni, "Photocatalytic degradation of methylene blue dye using Fe$_2$O$_3$/TiO$_2$ nanoparticles prepared by sol–gel method," *Journal of Alloys and Compounds,* vol. 553, pp. 19-29, 2013.

[17] X. Chen and S. S. Mao, "Titanium dioxide nanomaterials: synthesis, properties, modifications, and applications," *Chemical reviews,* vol. 107, no. 7, pp. 2891-2959, 2007.

[18] V. K. Gupta, R. Jain, A. Mittal, T. A. Saleh, A. Nayak, S. Agarwal, and S. Sikarwar, "Photo-catalytic degradation of toxic dye amaranth on TiO$_2$/UV in aqueous suspensions," *Materials science and engineering: C,* vol. 32, no. 1, pp. 12-17, 2012.

[19] A. Hu, R. Liang, X. Zhang, S. Kurdi, D. Luong, H. Huang, and M. R. Servos, "Enhanced photocatalytic degradation of dyes by TiO$_2$ nanobelts with hierarchical structures," *Journal of Photochemistry and Photobiology A: Chemistry,* vol. 256, pp. 7-15, 2013.

[20] A. M. Amanulla and R. Sundaram, "Green synthesis of TiO$_2$ nanoparticles using orange peel extract for antibacterial, cytotoxicity and humidity sensor applications," *Materials Today: Proceedings,* vol. 8, pp. 323-331, 2019.

[21] S. Alamdari, M. Sasani Ghamsari, C. Lee, W. Han, H. H. Park, M. J. Tafreshi, and M. H. M. Ara, "Preparation and characterization of zinc oxide nanoparticles using leaf extract of Sambucus ebulus," *Applied Sciences,* vol. 10, no. 10, p. 3620, 2020.

[22] K. G. Rao, C. Ashok, K. V. Rao, C. Chakra, and P. Tambur, "Green synthesis of TiO_2 nanoparticles using Aloe vera extract," *Int. J. Adv. Res. Phys. Sci,* vol. 2, no. 1A, pp. 28-34, 2015.

[23] S. Kaur, S. Rani, and R. K. Mahajan, "Adsorption kinetics for the removal of hazardous dye congo red by biowaste materials as adsorbents," *Journal of Chemistry,* vol. 2013, 2013.

[24] I. B. Bwatanglang, S. T. Magili, and I. Kaigamma, "Adsorption of phenol over bio-based silica/calcium carbonate (CS-SiO_2/$CaCO_3$) nanocomposite synthesized from waste eggshells and rice husks," *PeerJ Physical Chemistry,* vol. 3, p. 17, 2021.

[25] Z. Mi-Na, L. Xue-Pin, and S. Bi, "Adsorption of surfactants on chromium leather waste," *Journal-society of leather technologists and chemists,* vol. 90, no. 1, p. 1, 2006.

[26] N. Soliman and A. Moustafa, "Industrial solid waste for heavy metals adsorption features and challenges; a review," *Journal of Materials Research and Technology,* vol. 9, no. 5, pp. 10235-10253, 2020.

[27] B. Ekka, L. Rout, M. K. S. A. Kumar, R. K. Patel, and P. Dash, "Removal efficiency of Pb (II) from aqueous solution by 1-alkyl-3-methylimidazolium bromide ionic liquid mediated mesoporous silica," *Journal of Environmental Chemical Engineering,* vol. 3, no. 2, pp. 1356-1364, 2015.

[28] L. Wang, J. Li, Y. Jin, M. Chen, J. Luo, X. Zhu, and Y. Zhang, "Study on the removal of chromium (III) from leather waste by a two-step method," *Journal of Industrial and Engineering Chemistry,* vol. 79, pp. 172-180, 2019.

[29] S. Rizk and M. M. Hamed, "Batch sorption of iron complex dye, naphthol green B, from wastewater on charcoal, kaolinite, and tafla," *Desalination and Water Treatment,* vol. 56, no. 6, pp. 1536-1546, 2015.

[30] E. Bulut, M. Özacar, and İ. A. Şengil, "Equilibrium and kinetic data and process design for adsorption of Congo Red onto bentonite," *Journal of hazardous materials,* vol. 154, no. 1-3, pp. 613-622, 2008.

[31] H. Tun and C.-C. Chen, "Isosteric heat of adsorption from thermodynamic Langmuir isotherm," *Adsorption,* vol. 27, no. 6, pp. 979-989, 2021.

[32] G. Vijayakumar, M. Dharmendirakumar, S. Renganathan, S. Sivanesan, G. Baskar, and K. P. Elango, "Removal of Congo red from aqueous solutions by perlite," *Clean–soil, air, water,* vol. 37, no. 4-5, pp. 355-364, 2009.

[33] N. A. A. Salim, M. H. Puteh, M. H. Khamidun, M. A. Fulazzaky, N. H. Abdullah, A. R. M. Yusoff, M. Nuid, "Interpretation of isotherm models for adsorption of ammonium onto granular activated carbon," *Biointerface Res. Appl. Chem,* vol. 11, pp. 9227-9241, 2021.

[34] K. Allam, K. Gourai, A. El Bouari, B. Belhorma, and L. Bih, "Adsorption of Methylene Blue on raw and activated Clay: case study of Bengurir clay," *Journal of Materials and Environmental Science,* vol. 9, pp. 1750-1761, 2018.

[35] I. H. Ali, M. K. Al Mesfer, M. I. Khan, M. Danish, and M. M. Alghamdi, "Exploring adsorption process of lead (II) and chromium (VI) ions from aqueous solutions on acid activated carbon prepared from Juniperus procera leaves," *Processes,* vol. 7, no. 4, p. 217, 2019.

[36] S. S. Mohammed and D. T. Al-Heetimi, "Adsorption of Methyl Violet Dye from Aqueous Solution by Iraqi Bentonite and Surfactant–Modified Iraqi Bentonite," *Ibn AL-Haitham Journal For Pure and Applied Science,* vol. 32, no. 3, pp. 28-42, 2019.

[37] L. Lian, L. Guo, and C. Guo, "Adsorption of Congo red from aqueous solutions onto Ca-bentonite," *Journal of hazardous materials,* vol. 161, no. 1, pp. 126-131, 2009.

[38] M. Benjelloun, Y. Miyah, G. A. Evrendilek, F. Zerrouq, and S. Lairini, "Recent advances in adsorption kinetic models: their application to dye types," *Arabian Journal of Chemistry,* vol. 14, no. 4, p. 103031, 2021.

[39] S. Bentahar, A. Dbik, M. El Khomri, N. El Messaoudi, B. Bakiz, and A. Lacherai, "Study of removal of Congo red by local natural clay," *Scientific Study & Research. Chemistry & Chemical Engineering, Biotechnology, Food Industry,* vol. 17, no. 3, p. 295, 2016.